

AD-A043 871

TEXAS UNIV AT AUSTIN APPLIED RESEARCH LABS
QUARTERLY PROGRESS REPORT NUMBER 4, 1 APRIL - 30 JUNE 1972.(U)
SEP 72

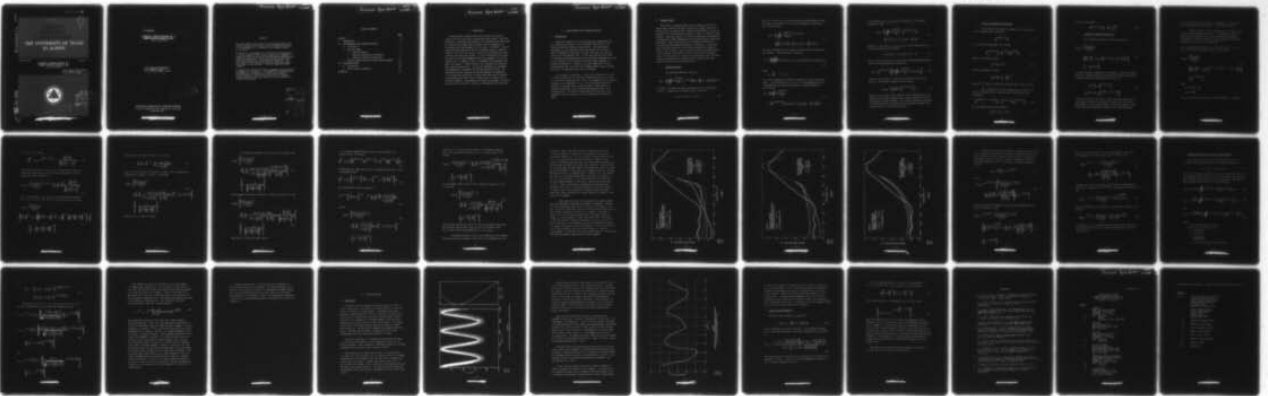
F/G 20/1

N00024-71-C-1266

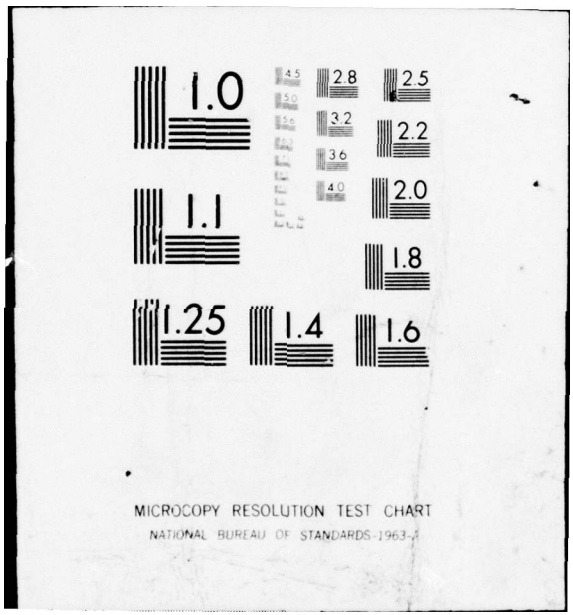
NL

UNCLASSIFIED

1 OF 1
AD
A043871



END
DATE
FILMED
9-77
DDC



MICROCOPY RESOLUTION TEST CHART
NATIONAL BUREAU OF STANDARDS-1963-A

002200

ADA 043871

(1)

B.S.

APPLIED RESEARCH LABORATORIES THE UNIVERSITY OF TEXAS AT AUSTIN

12 September 1972

Copy No. 1

QUARTERLY PROGRESS REPORT NO. 4
UNDER CONTRACT N00024-71-C-1266
1 April - 30 June 1972

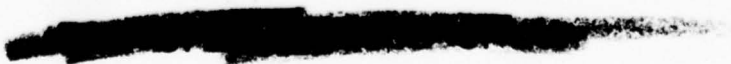
NAVAL SHIP SYSTEMS COMMAND
Contract N00024-71-C-1266
Proj. Ser. No. SF 11552002, Task 8118

002200 DDC FILE COPY:



DISTRIBUTION STATEMENT A
Approved for public release
Distribution Unlimited

DDC
RECEIVED
SEP 9 1972
A



11
12 September 1972

6
Number
QUARTERLY PROGRESS REPORT NO. 4
UNDER CONTRACT N00024-71-C-1266
1 April - 30 June 1972

12 40p.

15
NAVAL SHIP SYSTEMS COMMAND
Contract N00024-71-C-1266
Proj. Ser. No. SF 11552002, Task 8118

17
16 F11552

404 434

DISTRIBUTION STATEMENT A
Approved for public release
Distribution Unlimited

APPLIED RESEARCH LABORATORIES
THE UNIVERSITY OF TEXAS AT AUSTIN
AUSTIN, TEXAS 78712



6/8

ABSTRACT

This first quarter the reflection and scattering models were further developed, and a review of the literature preliminary to the development of a convergence zone propagation model was completed.

In Section II, the expansion of the heuristic scattering model to include composite (both large and small scale roughness) surface statistics is given which should improve backscattering predictive capabilities. This model does not include slope correction terms but has the advantage of simplicity. The more rigorous theoretical model which includes slope corrections terms is also expanded to allow for composite surface roughness.

A survey of the literature covering convergence zone propagation is summarized in Section III. An approach is outlined for the development of a convergence zone model using a Green's function expansion. This technique results in an ordered integral expansion where each integral can be associated with a particular multipath.

ACCESSION ID	
YES	World Section <input checked="" type="checkbox"/>
NO	Both Section <input type="checkbox"/>
BY	
DISTRIBUTION/AVAILABILITY CODES	
Dist	AVAIL. sec. or SPECIAL
A	

Folder on file

NOT
Preceding Page BLANK - FILMED

TABLE OF CONTENTS

	<u>Page</u>
ABSTRACT	iii
I. INTRODUCTION	1
II. BACKSCATTERING FROM COMPOSITE SURFACES	3
A. Introduction	3
B. Heuristic Model	4
1. Coherent Pressure	4
2. Composite Characteristic Functions	7
3. Incoherent Scattering Coefficient	8
C. Modified Fresnel Model with Exact Slope Treatment	23
III. CONVERGENCE ZONES	29
A. Introduction	29
B. Green's Function Expansion	33
REFERENCES	35

Preceding Page BLANK - NOT FILMED

I. INTRODUCTION

Work done under Contract N00024-71-C-1266 for the period of 1 April 1972 to 30 June 1972 is summarized in this report. This work represents a continuing investigation of the reflection and scattering of sound from the rough ocean boundaries, and the interaction of scattering with sound propagation in the ocean. In Section II the two scattering models derived at ARL are extended to apply to composite surfaces. This work will provide a basis for the prediction of back-scattering from the ocean surface. It will be shown that both large and small scale surface roughness effects are important in the back-scatter case. In addition, work on convergence zone propagation was begun this quarter. A brief survey of the literature was completed and is given in Section III. Theoretical treatments of convergence zone phenomena are discussed for both ray and wave theories. The limitations of both classical ray and wave methods are summarized. It was found that limitations of normal mode theory can be overcome by transforming the basic contour integral into an infinite sum of multipath integrals. The evaluation of these ray integrals is briefly discussed with an outline of future work dealing with this approach.

II. BACKSCATTERING FROM COMPOSITE SURFACES

A. Introduction

During this quarter the two scattering models developed at ARL were revised and extended to give theoretical predictions of the backscattering from composite rough surfaces. The simultaneous development of both scattering models was carried out in order to better understand the importance of phase, beam, and slope approximations in the backscatter case. It was found that the exact forms of the phase and beam approximations are relatively unimportant as long as the coherence of the scattered field near normal incidence is properly accounted for. However, it was also found that, for the backscattering case, the exact slope treatment must be used, and that the effects of shadowing should also be included.

The scattering coefficients, σ , used in this section are related to the usual definition of scattering strength through $S=4\sigma/A$, where A is the active scattering area. Here it is assumed that the scattering strength, S , is referenced to 1 yd. In the following section the heuristic (stationary phase) scattering model is developed from separate calculations of the coherent and incoherent parts of the scattered field. The modified Fresnel model with the exact slope treatment is given in Section C and is compared with the heuristic model.

B. Heuristic Model

The heuristic scattering model (given in detail in the final report under Contract N00024-69-C-1275 and in "Forward and Specular Scattering from a Rough Surface: Theory and Experiment", by Boyd and Deavenport¹) is here revised and extended to apply to composite rough surfaces. Particular emphasis is placed on improving the backscattering predictions without degrading the forward and specular scattering predictions. This subdivision will be divided into three parts following the chronological development of the model. In the first part a detailed derivation of the coherent pressure for composite surfaces will be given. The second part will give a brief discussion of the composite characteristic functions used in the scattering model. The third part will contain the development of the incoherent scattering coefficients for various surface statistics and some numerical results for the backscatter case.

1. Coherent Pressure

The scattered pressure is given by

$$P_s(\mathbf{r}) = \frac{ik}{2\pi} \iint_{\Sigma} \rho \frac{e^{ik(R_o + R_1)}}{R_o R_1} e^{-iky\zeta} \left(\frac{\partial \zeta}{\partial x} \hat{e}_x + \frac{\partial \zeta}{\partial y} \hat{e}_y - \hat{e}_z \right) \cdot \hat{e}_1 dx dy. \quad (1)$$

The various constants and ranges appearing in Eq. (1) are defined in Ref. 1. Assume that the surface height is given by

$$\zeta(x, y) = \zeta_1(x, y) + \zeta_2(x, y) \quad , \quad (2)$$

where $\zeta_1(x,y)$ and $\zeta_2(x,y)$ are random variables representing the large and small scale components of the surface roughness, respectively.

Eq. (1) then becomes

$$P_s(r) = \frac{ik}{2\pi} \iint_{\Sigma} \rho \frac{e^{ik(R_0+R_1)}}{R_0 R_1} e^{-ik\gamma(\zeta_1+\zeta_2)} \times \left[\left(\frac{\partial}{\partial x} (\zeta_1+\zeta_2) \right) \hat{e}_x + \frac{\partial}{\partial y} (\zeta_1+\zeta_2) \hat{e}_y - \hat{e}_z \right] \cdot \hat{e}_1 dx dy \quad (3)$$

The usual development of the coherent pressure can now be made using this equation. The mean pressure is given by

$$\langle P_s \rangle \equiv \iiint_{-\infty}^{\infty} \iiint_{-\infty}^{\infty} \iiint_{-\infty}^{\infty} P_s W_6(\zeta_1, \zeta_2, \zeta_{1x}, \zeta_{2x}, \zeta_{1y}, \zeta_{2y}) d\zeta_1 d\zeta_2 d\zeta_{1x} d\zeta_{2x} d\zeta_{1y} d\zeta_{2y} \quad (4)$$

where

$$\zeta_{1x} = \frac{\partial \zeta_1}{\partial x}, \text{ etc., and}$$

W_6 is the six-dimensional probability density of surface heights and slopes. Substituting Eq. (3) into Eq. (4), interchanging the order of integrations, and using the definition of the characteristic function gives

$$\langle P_s \rangle = \frac{ik}{2\pi} \iint_{\Sigma} \rho \frac{e^{ik(R_0+R_1)}}{R_0 R_1} \times \left\langle e^{-ik\gamma(\zeta_1+\zeta_2)} \left[(\zeta_{1x}+\zeta_{2x}) \hat{e}_x + (\zeta_{1y}+\zeta_{2y}) \hat{e}_y - \hat{e}_z \right] \cdot \hat{e}_1 \right\rangle dx dy \quad (5)$$

If the slopes $\zeta_{1x}, \zeta_{2x}, \zeta_{1y}, \zeta_{2y}$ and the heights ζ_1, ζ_2 are assumed independent, then

$$\langle P_s \rangle = \frac{ik}{2\pi} \iint_{\Sigma} \rho \frac{e^{ik(R_0+R_1)}}{R_0 R_1} \left\langle e^{-ik\gamma(\zeta_1+\zeta_2)} \hat{e}_1 \right\rangle \cdot \left\langle (\zeta_{1x}+\zeta_{2x})\hat{e}_x + (\zeta_{1y}+\zeta_{2y})\hat{e}_y - \hat{e}_z \right\rangle dx dy \quad (6)$$

Further, if the slopes $\zeta_{1x}, \zeta_{2x}, \zeta_{1y}, \zeta_{2y}$ are all zero-mean processes, then the expectation value becomes

$$\langle (\zeta_{1x}+\zeta_{2x})\hat{e}_x + (\zeta_{1y}+\zeta_{2y})\hat{e}_y - \hat{e}_z \rangle = -\hat{e}_z \quad (7)$$

Thus, if $\zeta_1(x,y)$ and $\zeta_2(x,y)$ are isotropic, the remaining expectation value can be removed from the integral and

$$\langle P_s \rangle = \left\langle e^{-ik\gamma(\zeta_1+\zeta_2)} \right\rangle \left[\frac{ik}{2\pi} \iint_{\Sigma} \rho \frac{e^{ik(R_0+R_1)}}{R_0 R_1} (\hat{e}_z \cdot \hat{e}_1) dx dy \right] \quad (8)$$

where the term in braces is the pressure reflected from a plane surface. The coherent intensity is then given by

$$\langle I_s \rangle_{\text{COH}} = \langle P_s \rangle \langle P_s \rangle^* = \left\langle e^{-ik\gamma(\zeta_1+\zeta_2)} \right\rangle^2 I_p \quad (9)$$

where I_p is the plane surface intensity and the other factor is the square of the composite characteristic function associated with the distribution of surface heights. The coherent scattering coefficient is obtained from this by dividing out the intensity scattered from a plane surface in the specular direction.

2. Composite Characteristic Functions

The one-dimensional composite characteristic function used in the scattering model is given by

$$\left\langle e^{-ik\gamma(\zeta_1 + \zeta_2)} \right\rangle . \quad (10)$$

If ζ_1 and ζ_2 are independent, this becomes

$$\left\langle e^{-ik\gamma(\zeta_1 + \zeta_2)} \right\rangle = \left\langle e^{-ik\gamma\zeta_1} \right\rangle \left\langle e^{-ik\gamma\zeta_2} \right\rangle , \quad (11)$$

where, for a Gaussian process

$$\left\langle e^{-ik\gamma\zeta} \right\rangle = e^{-g/2} , \quad (12)$$

and for an exponential process

$$\left\langle e^{-ik\gamma\zeta} \right\rangle = \left[1 + \frac{2g}{3} \right]^{-3/4} . \quad (13)$$

Here $g = k^2 \gamma^2 h^2$, where h is either the large or small scale rms height.

The two-dimensional composite characteristic functions can be treated similarly if the large and small scale processes are independent:

$$\left\langle e^{ik\gamma[(\zeta_1 + \zeta_2) - (\zeta'_1 + \zeta'_2)]} \right\rangle = \left\langle e^{ik\gamma(\zeta_1 - \zeta'_1)} \right\rangle \left\langle e^{ik\gamma(\zeta_2 - \zeta'_2)} \right\rangle . \quad (14)$$

For the Gaussian bivariate distribution

$$\left\langle e^{ik\gamma(\zeta - \zeta')} \right\rangle = e^{-g(1-c)} , \quad (15)$$

and for the exponential

$$\langle e^{ik\gamma(\zeta-\zeta')} \rangle = \left[1 + \frac{2g}{3}(1-c) \right]^{-3/2} \quad (16)$$

3. Incoherent Scattering Coefficient

The incoherent scattering coefficient is given by

$$\begin{aligned} \sigma_{\text{INCOH}} &= \frac{AF^2(r_{00}+r_{10})^2}{\gamma^2 r_{00}^2 r_{10}^2} \\ &\times \left\{ \frac{k^2 \gamma^2}{2\pi} \int_0^\infty J_0(V_{xy}r) \left[\langle e^{ik\gamma(\zeta-\zeta')} \rangle - \langle e^{-ik\gamma\zeta} \rangle^2 \right] r dr \right\} \quad (17) \\ &\times \left[1 - \rho^2 \langle e^{-ik\gamma\zeta} \rangle^2 \right] . \end{aligned}$$

An initial attempt at adapting this expression to composite surfaces consists of simply replacing the characteristic functions with their equivalent composite characteristic functions, i.e.,

$$\begin{aligned} \langle e^{-ik\gamma\zeta} \rangle &\rightarrow \langle e^{-ik\gamma(\zeta_1+\zeta_2)} \rangle \\ \langle e^{ik\gamma(\zeta-\zeta')} \rangle &\rightarrow \langle e^{ik\gamma[(\zeta_1+\zeta_2)-(\zeta'_1+\zeta'_2)]} \rangle . \end{aligned} \quad (18)$$

It should be noted at the outset, however, that this approach is an approximation in that no modification is made to the slope terms which appear in the original integral for the total pressure. These slope terms have already been evaluated at the stationary phase

points and removed from the integral as Beckmann's F. The effect of this approximation will be examined in the following section.

Equation (17) will here be developed for (a) Gaussian large and small scale distribution functions, (b) exponential large and small scale distributions, and (c) mixed Gaussian and exponential distributions. Forms for both Gaussian and exponential correlation functions will be given in all three cases.

(a) For Gaussian large and small scale processes, Eqs. (11), (12), (14), (15), and (18) are used so that Eq. (17) becomes

$$\sigma_{\text{INCOH}} = \frac{AF^2(r_{00}+r_{10})^2}{\gamma^2 r_{00}^2 r_{10}^2} \quad (19)$$

$$\times \left\{ \frac{k^2 \gamma^2}{2\pi} \int_0^\infty J_0(v_{xy}r) \left[e^{-g_1(1-c_1)} e^{-g_2(1-c_2)} - e^{-g_1} e^{-g_2} \right] r dr \right\}$$

$$\times \left[1 - \rho^2 e^{-(g_1+g_2)} \right],$$

where

$$g_1 = k^2 \gamma^2 h_1^2, \text{ and}$$

$$g_2 = k^2 \gamma^2 h_2^2$$

and h_1, h_2 are the large and small scale rms heights. To evaluate

Eq. (19) the characteristic function must be expanded in terms of the large and small scale correlation functions c_1 and c_2 :

$$\begin{aligned} \left\langle e^{iky \left[(\zeta_1 + \zeta_2) - (\zeta'_1 + \zeta'_2) \right]} \right\rangle &= e^{-[g_1(1-c_1) + g_2(1-c_2)]} \\ &= e^{-(g_1+g_2)} e^{g_1 c_1 + g_2 c_2} \end{aligned} \quad (20)$$

Thus, $e^{g_1 c_1 + g_2 c_2}$ must be expanded in a series in terms of c_1 and c_2 where the first term is required to be unity:

$$\begin{aligned} e^{g_1 c_1 + g_2 c_2} &= e^{g_1 c_1} e^{g_2 c_2} = \left(\sum_{n=0}^{\infty} \frac{g_1^n c_1^n}{n!} \right) \left(\sum_{j=0}^{\infty} \frac{g_2^j c_2^j}{j!} \right) \\ &= \sum_{j=0}^{\infty} \sum_{n=0}^{\infty} \frac{g_1^n g_2^j}{j! n!} c_1^n c_2^j, \end{aligned} \quad (21)$$

where the $j=0, n=0$ term is 1. Thus the integral becomes

$$\sigma_{\text{INCOH}} = \frac{AF^2 (r_{00} + r_{10})^2}{\gamma^2 r_{00}^2 r_{10}^2} \quad (22)$$

$$\times \left\{ \frac{k^2 \gamma^2}{2\pi} e^{-(g_1+g_2)} \sum_{j=0}^{\infty} \sum_{n=0}^{\infty} \frac{g_1^n g_2^j}{j! n!} \int_0^{\infty} J_0(v_{xy} r) c_1^n c_2^j r dr \right\} \left[1 - \rho^2 e^{-(g_1+g_2)} \right]$$

where the $j=0, n=0$ term of the sum is omitted. The integral to be evaluated is

$$\int_0^{\infty} J_0(v_{xy} r) c_1^n c_2^j r dr \quad (23)$$

where c_1 and c_2 are the large and small scale correlation functions, respectively. For Gaussian correlation functions

$$c_1(r) = e^{-r^2/l_1^2}$$

and

$$c_2(r) = e^{-r^2/l_2^2},$$

(24)

where l_1 and l_2 are the large and small scale correlation lengths. Equation (23) becomes

$$\int_0^\infty J_0(v_{xy}r) e^{-[n/l_1^2 + j/l_2^2]r^2} r dr \quad (25)$$

Performing this integral and substituting the result into Eq. (22) gives (for Gaussian distributions and correlation)

$$\begin{aligned} \sigma_{\text{INCOH}} &= \frac{AF^2(r_{00} + r_{10})^2 k^2}{2\pi r_{00} r_{10}} e^{-(g_1 + g_2)} \\ &\times \sum_{j=0}^{\infty} \sum_{n=0}^{\infty} \frac{g_1^n g_2^j e^{-v_{xy}^2/4[n/l_1^2 + j/l_2^2]}}{n! j! 2^{\binom{n+j}{2}} \begin{pmatrix} n & j \\ l_1 & l_2 \end{pmatrix}} \left[1 - \rho^2 e^{-(g_1 + g_2)} \right] \end{aligned} \quad (26)$$

For exponential correlation functions

$$c_1(r) = e^{-r/l_1},$$

and

$$c_2(r) = e^{-r/l_2},$$

(27)

so that Eq. (23) becomes

$$\int_0^{\infty} J_0(v_{xy}r) e^{-\left[\frac{n}{l_1} + \frac{j}{l_2}\right]r} r dr = \frac{\left(\frac{n}{l_1} + \frac{j}{l_2}\right)}{\left[\left(\frac{n}{l_1} + \frac{j}{l_2}\right)^2 + v_{xy}^2\right]^{3/2}} \quad (28)$$

Thus for Gaussian large and small scale distribution functions and exponential large and small scale correlation functions, the incoherent scattering coefficient is

$$\sigma_{\text{INCOH}} = \frac{AF^2(r_{00}+r_{10})^2 k^2}{2\pi r_{00}^2 r_{10}^2} e^{-(g_1+g_2)} \sum_{n=0}^{\infty} \sum_{j=0}^{\infty} \frac{g_1^n g_2^j}{n!j!} \frac{\left(\frac{n}{l_1} + \frac{j}{l_2}\right)}{\left[\left(\frac{n}{l_1} + \frac{j}{l_2}\right)^2 + v_{xy}^2\right]^{3/2}} \quad (29)$$

(b) For exponential large and small scale distribution functions Eqs. (11), (13), (14), (16), and (18) are used in Eq. (17) so that

$$\sigma_{\text{INCOH}} = \frac{AF^2(r_{00}+r_{10})^2}{\gamma^2 r_{00}^2 r_{10}^2} \times \left\{ \frac{k^2 \gamma^2}{2\pi} \int_0^{\infty} J_0(v_{xy}r) \left\{ \left[1 + \frac{2g_1}{3}(1-c_1) \right] \left[1 + \frac{2g_2}{3}(1-c_2) \right] \right\}^{-3/2} - \left\{ \left[1 + \frac{2g_1}{3} \right] \left[1 + \frac{2g_2}{3} \right] \right\}^{-3/2} \right\} r dr \quad (30)$$

$$\times \left[1 - \rho^2 \left\{ \left[1 + \frac{2g_1}{3} \right] \left[1 + \frac{2g_2}{3} \right] \right\}^{-3/2} \right]$$

The characteristic function expansion is given by

$$\left[1 + \frac{2g}{3}(1-c)\right]^{-3/2} = \sum_{n=0}^{\infty} \frac{(2n+1)!! g^n c^n}{3^n n! \left(1 + \frac{2g}{3}\right)^{n+3/2}} \quad (31)$$

Again, the first term of the expansion is equal to the one-dimensional characteristic function so that Eq. (30) becomes

$$\sigma_{\text{INCOH}} = \left\{ \frac{AF^2 (r_{00} + r_{10})^2 k^2}{2\pi r_{00}^2 r_{10}^2} \right. \quad (32)$$

$$\times \sum_{n=0}^{\infty} \sum_{j=0}^{\infty} \frac{(2n+1)!! (2j+1)!! g_1^n g_2^j}{3^{n+j} n! j! \left(1 + \frac{2g_1}{3}\right)^{n+3/2} \left(1 + \frac{2g_2}{3}\right)^{j+3/2}} \int_0^{\infty} J_0(v_{xy} r) c_1^n c_2^j r dr \left. \right\}$$

$$\times \left[1 - \frac{\rho^2}{\left[\left(1 + \frac{2g_1}{3}\right)\left(1 + \frac{2g_2}{3}\right)\right]^{3/2}} \right]$$

where the $n=0, j=0$ term is omitted.

For Gaussian correlation functions Eq. (25) is used so that

$$\sigma_{\text{INCOH}} = \left\{ \frac{AF^2(r_{00}+r_{10})^2 k^2}{2\pi r_{00}r_{10}} \times \sum_{n=0}^{\infty} \sum_{j=0}^{\infty} \frac{(2n+1)!!(2j+1)!! g_1^n g_2^j e^{v_{xy}^2/4 \left[\frac{n}{l_1} + \frac{j}{l_2} \right]^2}}{2 \cdot 3^{n+j} n! j! \left[\frac{n}{l_1} + \frac{j}{l_2} \right] \left(1 + \frac{2g_1}{3}\right)^{n+3/2} \left(1 + \frac{2g_2}{3}\right)^{j+3/2}} \right\} \quad (33)$$

$$\times \left[1 - \frac{\rho^2}{\left[\left(1 + \frac{2g_1}{3}\right) \left(1 + \frac{2g_2}{3}\right) \right]^{3/2}} \right]$$

For exponential correlation functions Eq. (28) is used in Eq. (32) and

$$\sigma_{\text{INCOH}} = \left\{ \frac{AF^2(r_{00}+r_{10})^2 k^2}{2\pi r_{00}r_{10}} \times \sum_{n=0}^{\infty} \sum_{j=0}^{\infty} \frac{(2n+1)!!(2j+1)!! g_1^n g_2^j \left(\frac{n}{l_1} + \frac{j}{l_2} \right)}{3^{n+j} n! j! \left(1 + \frac{2g_1}{3}\right)^{n+3/2} \left(1 + \frac{2g_2}{3}\right)^{j+3/2} \left[\left(\frac{n}{l_1} + \frac{j}{l_2} \right)^2 + v_{xy}^2 \right]^{3/2}} \right\} \quad (34)$$

$$\times \left[1 - \frac{\rho^2}{\left[\left(1 + \frac{2g_1}{3}\right) \left(1 + \frac{2g_2}{3}\right) \right]^{3/2}} \right],$$

where the $n=0, j=0$ term is again omitted.

(c) Assuming independent large and small scale processes, the integral in Eq. (17) becomes

$$\int_0^\infty J_0(v_{xy}r) \left[\langle e^{iky(\zeta_1 - \zeta'_1)} \rangle \langle e^{iky(\zeta_2 - \zeta'_2)} \rangle - \langle e^{-iky\zeta_1} \rangle \langle e^{-iky\zeta_2} \rangle \right] r dr . \quad (35)$$

Assuming that the large scale process is Gaussian and the small scale is exponential gives

$$\int_0^\infty J_0(v_{xy}r) \left\{ e^{-g_1(1-c_1)} \left[1 + \frac{2g_2}{3}(1-c_2) \right]^{-3/2} - e^{-g_1} \left[1 + \frac{2g_2}{3} \right]^{-3/2} \right\} r dr . \quad (36)$$

The characteristic function expansion is

$$e^{-g_1(1-c_1)} \left[1 + \frac{2g_2}{3}(1-c_2) \right]^{-3/2} = e^{-g_1} \sum_{j=0}^{\infty} \sum_{n=0}^{\infty} \frac{g_1^j c_1^j}{j!} \frac{(2n+1)!! g_2^n c_2^n}{3^n n! \left(1 + \frac{2g_2}{3} \right)^{n+3/2}} , \quad (37)$$

so that

$$\begin{aligned} \sigma_{\text{INCOH}} &= \left\{ \frac{AF^2 (r_{00} + r_{10})^2 k^2}{2\pi r_{00}^2 r_{10}^2} e^{-g_1} \right. \\ &\times \left. \sum_{j=0}^{\infty} \sum_{n=0}^{\infty} \frac{(2n+1)!! g_1^j g_2^n}{j! n! 3^n \left(1 + \frac{2g_2}{3} \right)^{n+3/2}} \int_0^\infty J_0(v_{xy}r) c_1^j c_2^n r dr \right\} \\ &\times \left[1 - \rho^2 e^{-g_1} \left[1 + \frac{2g_2}{3} \right]^{-3/2} \right] . \end{aligned} \quad (38)$$

where the $n=0, j=0$ term is again omitted. For Gaussian large and small scale correlation functions, Eq. (25) is used, and Eq. (38) becomes

$$\sigma_{\text{INCOH}} = \frac{AF^2(r_{00}+r_{10})^2 k^2}{2\pi r_{00}^2 r_{10}^2} e^{-g_1} \sum_{j=0}^{\infty} \sum_{n=0}^{\infty} \frac{(2n+1)!! g_1^j g_2^n e^{-v_{xy}^2/4 [j/l_1^2 + n/l_2^2]}}{2 \cdot j! n! 3^n \left(1 + \frac{2g_2}{3}\right)^{n+3/2} \left[\frac{j+n}{l_1^2 l_2^2}\right]} \times \left[1 - \rho^2 e^{-g_1} \left[1 + \frac{2g_2}{3}\right]^{-3/2}\right] \quad (39)$$

For exponential large and small scale correlation functions Eq. (28) is used, and

$$\sigma_{\text{INCOH}} = \left\{ \frac{AF^2(r_{00}+r_{10})^2 k^2}{2\pi r_{00}^2 r_{10}^2} e^{-g_1} \times \sum_{j=0}^{\infty} \sum_{n=0}^{\infty} \frac{(2n+1)!! g_1^j g_2^n}{j! n! 3^n \left(1 + \frac{2g_2}{3}\right)^{n+3/2}} \frac{\left(\frac{j+n}{l_1^2 l_2^2}\right)}{\left(\left[\frac{j+n}{l_1^2 l_2^2}\right]^2 + v_{xy}^2\right)^{3/2}} \right\} \times \left[1 - \rho^2 e^{-g_1} \left[1 + \frac{2g_2}{3}\right]^{-3/2}\right] \quad (40)$$

The incoherent scattering coefficients for an exponential large scale process and a Gaussian small scale process can be obtained from Eqs. (39) and (40) by interchanging (g_1, l_1) and (g_2, l_2) .

Preliminary numerical results were obtained from the formulas given above and were compared to data taken at one frequency from the

smoothest of ARL's rough model surfaces. The data were taken at 100 kHz from Surface I, which has an rms height of 0.091 in. and correlation lengths of 1.4 in. for Gaussian correlation functions and 2.55 in. for exponential correlation functions. Figure 1 shows results for Gaussian large and small scale distribution functions with Gaussian large and small scale correlation functions. From the graph, it is obvious that the basic shape of the theoretical curves is correct and that the addition of the small scale roughness gives the necessary flattening effect at low grazing angles. However, it is also obvious that the fit to the experimental data is not good in the region of 50 to 80° grazing angle. It is believed that this is in part due to the approximate treatment of the slopes. Similar results are seen in Fig. 2, using an exponential distribution for the large scale roughness, and in Fig. 3, using an exponential correlation function. In addition, use of the exponential correlation causes the large values near normal incidence and somewhat obscures the effects of the small scale roughness.

The slight rise in all of the curves at low grazing angles would be eliminated by including the effects of shadowing. Although for some of the cases shown, the fit of theory to experiment is not bad, it should be noted that there are two major factors which indicate that further refinement of the theory is necessary. The first of these factors is that fairly large values of the small scale rms height, σ_2 , were necessary to produce the curves shown. The second is that the overall k^4 frequency dependence will not allow fits to be made to the data at other frequencies without significantly changing the values of the input statistical parameters. It will be shown that both of these problems can be attributed, in part, to the slope approximations. In the next section the Fresnel model will be developed for composite surfaces using the exact slope treatment.

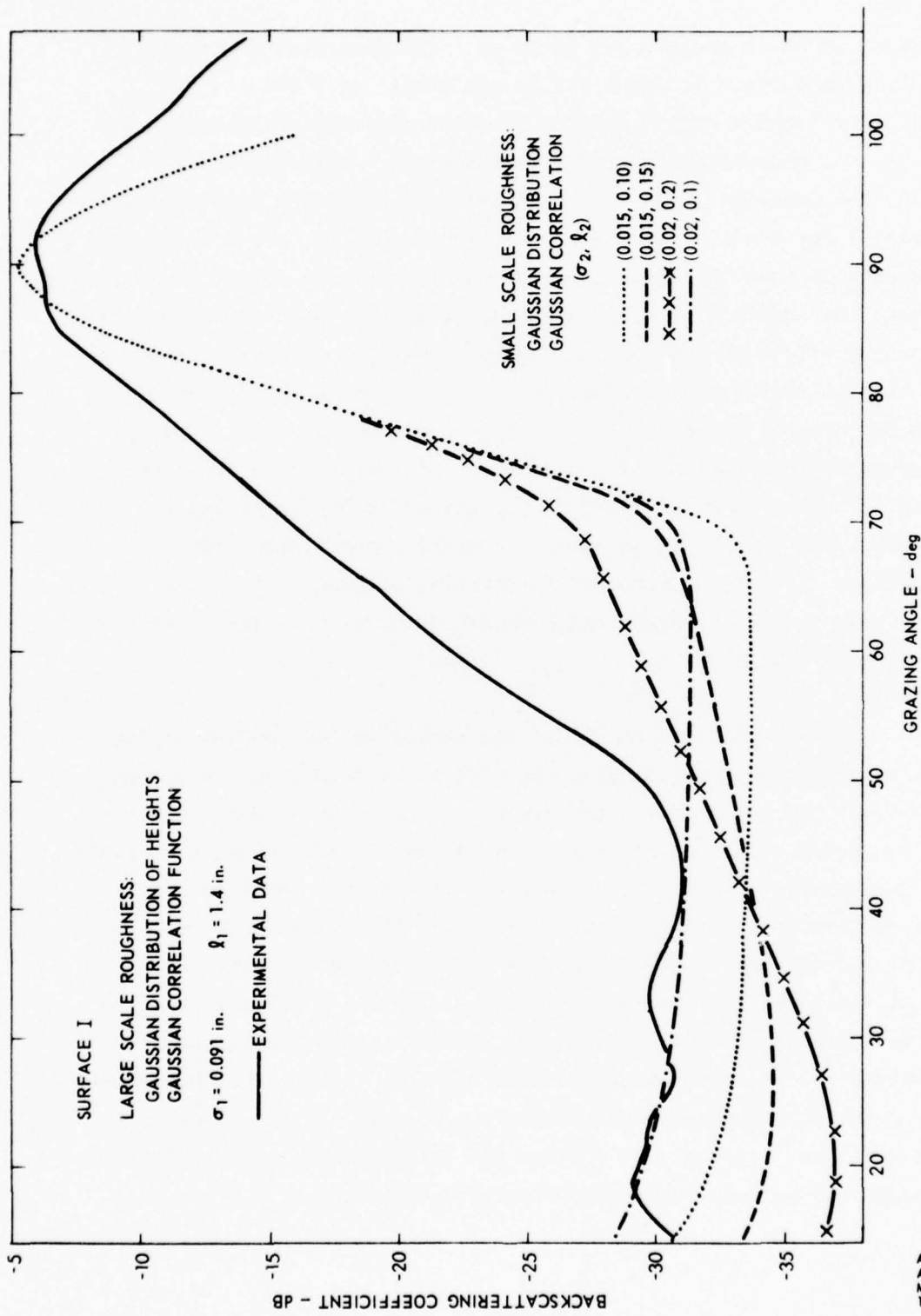


FIGURE 1

ARL - UT
 AS-72-1160
 MLB - DR
 10 - 5 - 72

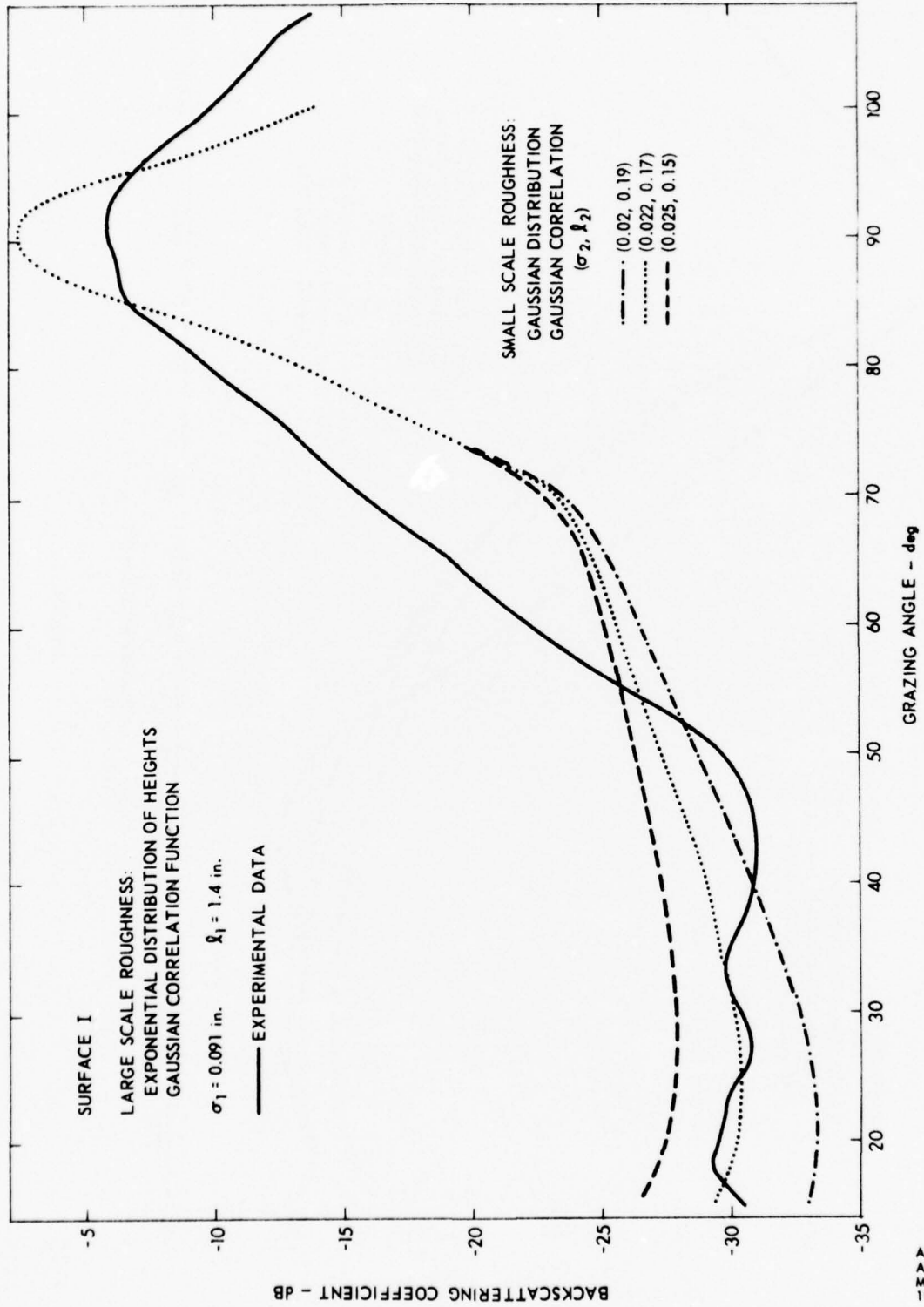


FIGURE 2

ARL - UT
AS-72-1161
MLB - DR
10-5-72

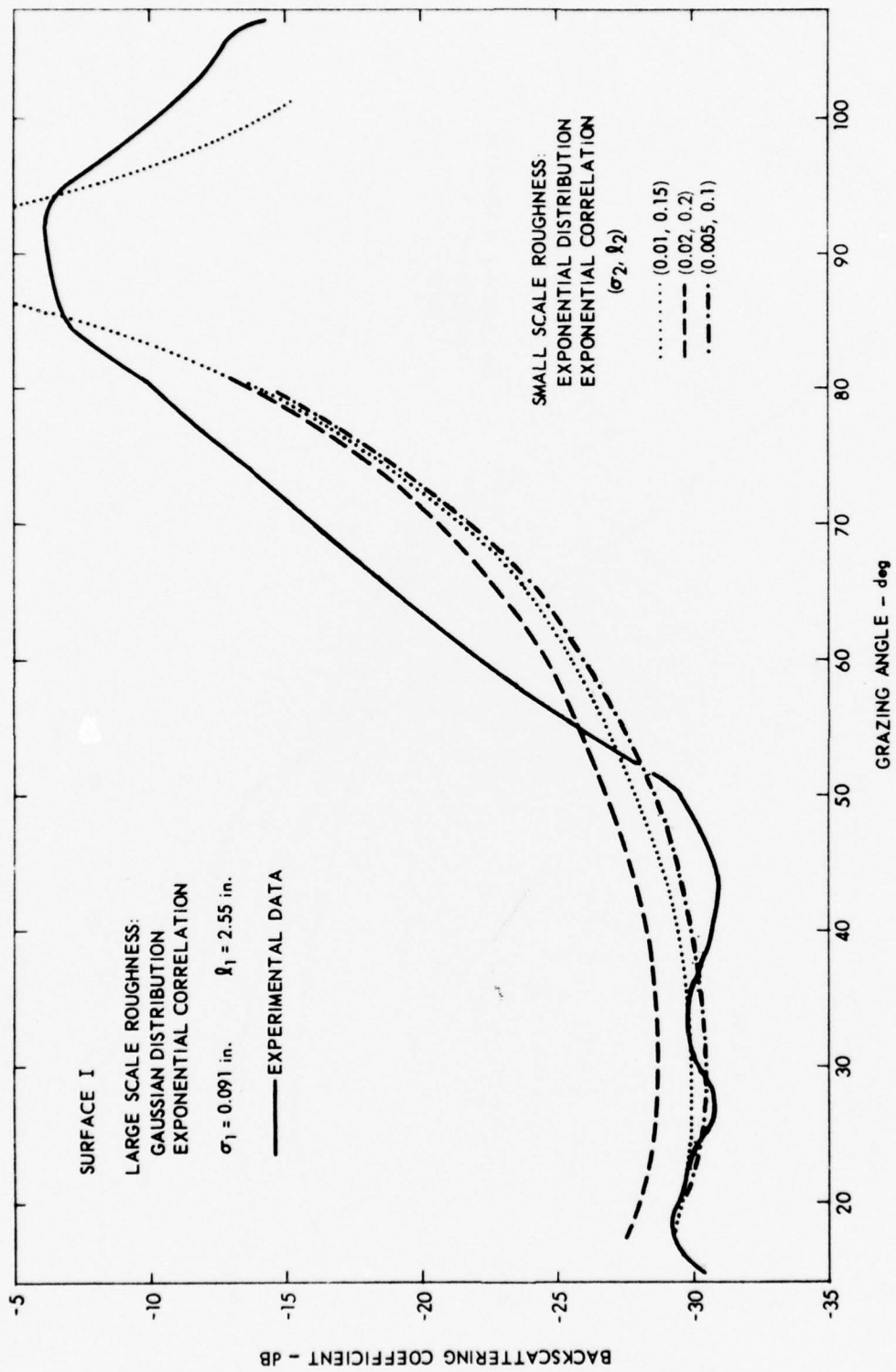


FIGURE 3

ARL - UT
 AS - 72 - 1162
 MLB - DR
 10 - 5 - 72

The total scattering coefficient for Gaussian large and small scale distributions and Gaussian correlation functions will now be put into a form that is easily compared with the results of the Fresnel model given in the next section. The total scattering coefficient is obtained by adding Eq. (26) to the coherent scattering coefficient given by

$$\sigma_{\text{COH}} = \frac{\langle I_s \rangle_{\text{COH}}}{I_p} = \rho^2 e^{-(g_1+g_2)}, \quad (41)$$

so that

$$\sigma_{\text{TOTAL}} = \rho^2 e^{-(g_1+g_2)} + \left\{ \frac{AF^2(r_{00}+r_{10})^2 k^2}{2\pi r_{00}^2 r_{10}^2} e^{-(g_1+g_2)} \right. \\ \left. \times \sum_{i=0}^{\infty} \sum_{j=0}^{\infty} \frac{g_1^i g_2^j}{i! j!} e^{-v_{xy}^2/4 \left[i/l_1^2 + j/l_2^2 \right]} \frac{1}{2 \binom{i+j}{l_1 \quad l_2}} \right\} \left[1 - \rho^2 e^{-(g_1+g_2)} \right]. \quad (42)$$

If $g_1 \gg 1$ and $g_2 \ll 1$, the summation over j can be replaced by the two lowest order terms, so that

$$\sigma_{\text{TOTAL}} = \rho^2 e^{-(g_1+g_2)} + \frac{AF^2(r_{00}+r_{10})^2 k^2}{2\pi r_{00}^2 r_{10}^2} e^{-(g_1+g_2)} \\ \times \left\{ \sum_{i=0}^{\infty} \frac{g_1^i l_1^2}{i!} \frac{e^{-v_{xy}^2 l_1^2/4i}}{2i} + \sum_{i=0}^{\infty} \frac{g_1^i}{i!} g_2 \frac{e^{-v_{xy}^2/4 \left[i/l_1^2 + 1/l_2^2 \right]}}{2 \binom{i+1}{l_1 \quad l_2}} \right\} \\ \times \left[1 - \rho^2 e^{-(g_1+g_2)} \right]. \quad (43)$$

However, the first summation is the incoherent part for the large scale roughness alone with an extra factor of e^{-g_2} , so that

$$\sigma_{\text{TOTAL}} = e^{-g_2} \sigma_1 + e^{-g_2} \frac{AF^2(r_{00}+r_{10})^2 k^2}{2\pi r_{00}^2 r_{10}^2} e^{-g_1} \times \sum_{i=0}^{\infty} g_2 \frac{g_1^i}{i!} \frac{e^{-v_{xy}^2/4} \left[i/l_1^2 + 1/l_2^2 \right]}{2 \binom{i+1}{l_1} \binom{i}{l_2}} \left[1 - \rho^2 e^{-(g_1+g_2)} \right] \quad (44)$$

Assuming that $l_1 \gg l_2$, restriction of the formula to the backscatter case where the coherence, $(\rho^2 e^{-(g_1+g_2)})$, is negligible gives the simple form

$$\sigma_{\text{TOTAL}} = e^{-g_2} \sigma_1 + \frac{AF^2(r_{00}+r_{10})^2 k^2}{2\pi r_{00}^2 r_{10}^2} e^{-g_2} \frac{l_2^2}{2} e^{-v_{xy}^2 l_2^2/4} g_2 \quad (45)$$

Since $g_2 = k^2 \gamma^2 h_2^2$ and, for backscatter $\gamma = 2 \sin \theta r$ and $F = 1/\sin \theta r$, Eq. (45) becomes

$$\sigma_{\text{TOTAL}} = e^{-g_2} \sigma_1 + \frac{A(r_{00}+r_{10})^2}{2\pi r_{00}^2 r_{10}^2} e^{-g_2} \left(2k^4 h_2^2 l_2^2 \right) e^{-v_{xy}^2 l_2^2/4} \quad (46)$$

This equation will be compared with the results of the Fresnel model in the next section in order to determine the effects of the slope approximations.

C. Modified Fresnel Model with Exact Slope Treatment

It has been shown previously¹ that the expression for the scattered intensity developed from Eq. (1) may be expressed as

$$\langle I_s \rangle = \langle I_s \rangle_0 + \langle I_s \rangle_1 + \langle I_s \rangle_2 \quad (47)$$

where the "0" subscript indicates the zero slope term, and the "1" and "2" subscripted terms arise as a result of the exact slope treatment. When a realistic beam approximation and Fresnel phase approximation is made, the individual terms in Eq. (47) are given by

$$\langle I_s \rangle_0 = k^2 \sin^2 \theta_r \Gamma \iint_{-\infty}^{+\infty} e^{-(Mx^2 + Ny^2)} e^{ikax} \left\langle e^{-ik\gamma(\zeta - \zeta')} \right\rangle dx dy \quad , \quad (48)$$

$$\langle I_s \rangle_1 = -\frac{\cos^2 \theta_r}{\gamma^2} \Gamma \iint_{-\infty}^{+\infty} e^{-(Mx^2 + Ny^2)} e^{ikax} \frac{\partial^2}{\partial x^2} \left\langle e^{-ik\gamma(\zeta - \zeta')} \right\rangle dx dy \quad , \quad (49)$$

and

$$\langle I_s \rangle_2 = i \frac{k \sin \theta_r \cos \theta_r}{\gamma} \Gamma \iint_{-\infty}^{+\infty} e^{-(Mx^2 + Ny^2)} e^{ikax} \frac{\partial}{\partial x} \left\langle e^{-ik\gamma(\zeta - \zeta')} \right\rangle dx dy \quad , \quad (50)$$

where

θ_r is the receiver grazing angle,

θ_i is the source grazing angle,

$$\gamma = \sin \theta_i + \sin \theta_r,$$

$$a = \cos \theta_i - \cos \theta_r,$$

$$\Gamma = \frac{A}{2K(2\pi r_{00} r_{10})^2},$$

$A = \pi \alpha \beta$; the elliptical insonified area,

k is the wave number,
 r_{00} is the surface to source distance,
 r_{10} is the surface to receiver distance,
 $K = 3/(20 \log_{10} e)$, a beam parameter,
 $R = 2r_{00}r_{10}/(r_{00}+r_{10})$,
 $R_1 = 2r_{00}r_{10}/(r_{00}\sin^2\theta_r + r_{10}\sin^2\theta_1)$,
 $M = k^2\alpha^2/2KR_1^2 + K/2\alpha^2$,
 $N = k^2\beta^2/2KR^2 + K/2\beta^2$,

and $\langle e^{-ik\gamma(\zeta-\zeta')} \rangle$ represents the average intensity modulation due to the surface roughness.

For a Gaussian distributed surface with two independent roughness scales, the characteristic function is given by Eq. (20)

$$\left\langle e^{-ik\gamma[(\zeta_1+\zeta_2)-(\zeta'_1+\zeta'_2)]} \right\rangle = e^{-g_1(1-c_1)} e^{-g_2(1-c_2)}, \quad (51)$$

where

$$g_1 = k^2\gamma^2 h_1^2,$$

$$g_2 = k^2\gamma^2 h_2^2,$$

h_1 is the rms value of the large scale roughness,

h_2 is the rms value of the small scale roughness, and

c_2, c_1 are the normalized surface autocorrelation functions for the two scales of roughness.

In order to insure that the results will be simple we shall make two assumptions:

$$g_1 \gg 1$$

and

$$g_2 \ll 1$$

(52)

With these assumptions we may make the "large g " approximation in the large scale characteristic function,

$$e^{-g_1(1-c_1)} \cong e^{-g_1 |c_1''(0)| (x^2+y^2)} \quad (53)$$

and the "small g " approximation in the small scale characteristic function,

$$e^{-g_2(1-c_2)} \cong e^{-g_2 (1+g_s c_s)} \quad (54)$$

To a reasonable approximation, c_1 is given by a Gaussian correlation function. Since no physical knowledge of the small scale roughness is available, it will be arbitrarily assumed that it is also Gaussian; thus

$$\begin{aligned} \langle \rangle &= e^{-g_1(x^2+y^2)/l_1^2 - g_2} + g_2 e^{-\left(g_1/l_1^2 + 1/l_2^2\right)(x^2+y^2) - g_2} \\ &\approx e^{-g_1(x^2+y^2)/l_1^2 - g_2} + g_2 e^{-(x^2+y^2)/l_2^2 - g_2}, \end{aligned} \quad (55)$$

In Eq. (55) it has been assumed $1/l_2^2 \gg g_1/l_1^2$, which means that for moderately large frequencies the slopes of the small scale roughness must be much larger than those of the large scale roughness.

Additional quantities which are required for Eqs. (48) through (50) are

$$\frac{\partial}{\partial x} \langle \rangle = -2g_1/l_1^2 x e^{-g_1(x^2+y^2)/l_1^2 - g_2} - 2g_2/l_2^2 x e^{-(x^2+y^2)/l_2^2 - g_2} \quad (56)$$

and

$$\begin{aligned} \frac{\partial^2}{\partial x^2} \langle \rangle = & \left[-2g_1/l_1^2 + 4(g_1/l_1^2)^2 x^2 \right] e^{-g_1/l_1^2(x^2+y^2)-g_2} \\ & + \left[-2g_2/l_2^2 + 4g_2/l_2^4 x^2 \right] e^{-(x^2+y^2)/l_2^2-g_2} \end{aligned} \quad (57)$$

Substitutions of Eqs. (55), (56), and (57) into Eqs. (48), (49), and (50), respectively, and the subsequent integrations yield

$$\langle I_s \rangle_0 = e^{-g_2} k^2 \sin^2 \theta_r \pi \Gamma \left[\frac{e^{-k^2 a^2 / 4(M+g_1/l_1^2)}}{\sqrt{(M+g_1/l_1^2)(N+g_1/l_1^2)}} \right] + \left\{ g_2 l_2^2 e^{-k^2 a^2 l_2^2 / 4} \right\}, \quad (58)$$

$$\begin{aligned} \langle I_s \rangle_1 = & e^{-g_2} \frac{\cos^2 \theta_r}{\gamma^2} \pi \Gamma \left[\frac{g_1/l_1^2 \left[2M(M+g_1/l_1^2) + g_1 k^2 a^2 / l_1^2 \right] e^{-k^2 a^2 / 4(M+g_1/l_1^2)}}{\sqrt{(M+g_1/l_1^2)^5 (N+g_1/l_1^2)}} \right] \\ & + \left\{ g_2 \left(2 + 1/2 l_2^2 k^2 a^2 \right) e^{-k^2 a^2 l_2^2 / 4} \right\}, \end{aligned} \quad (59)$$

and

$$\begin{aligned} \langle I_s \rangle_2 = & e^{-g_s} \frac{k \sin 2\theta_r}{\gamma} \pi \Gamma \left[\frac{g_1/l_1^2 k a e^{-k^2 a^2 / 4(M+g_1/l_1^2)}}{\sqrt{(M+g_1/l_1^2)^3 (N+g_1/l_1^2)}} \right] \\ & + \left\{ g_2 l_2^2 k a e^{-k^2 a^2 l_2^2 / 4} \right\} \end{aligned} \quad (60)$$

Now defining the scattering coefficient in the usual manner, $\sigma = \langle I_2 \rangle \left(\frac{r_{00} + r_{10}}{2} \right)^2$, examination of the first terms in the brackets in Eqs. (58), (59), and (60) reveals that these are the terms which arise solely from the large scale roughness, except for the factor e^{-g_2} . The terms in the second set of brackets arise solely from the small scale roughness. Regrouping terms, simplifying, and denoting the large scale scattering coefficient by σ_1 , the scattering coefficient obtained from Eqs. (58), (59), and (60) becomes

$$\sigma = e^{-g_2} \sigma_1 + e^{-g_2} \frac{A(r_{00} + r_{10})^2}{2\pi r_{00} r_{10}} \frac{1}{2K} \left(2k^4 h_2^2 \right) e^{-v_{xy}^2 / 4} \quad (61)$$

The scattering coefficient given by Eq. (61) contains several interesting features. First, the coefficient may be represented as the sum of the effects due to the large and small roughness. For most frequencies of interest, $e^{-g_2} \approx 1$; thus the two effects are practically independent of one another. Secondly, the angular dependence of the two effects is markedly different. The scattering coefficient for the large scale roughness, σ_1 , starts out at relatively high levels and decreases rapidly with decreasing grazing angles, while the small scale scattering effect is essentially constant at the low grazing angles where it becomes dominant. Finally, it should be noted that the heuristic model and the modified Fresnel model of the scattering process give identical results for the small scale scattering. This is because these models differ only in their treatment of the incoherent component near the specular direction. When the incoherent component dominates, as in the case of small angle backscattering, the results of the two models are equivalent, thereby confirming the suitability of the Fraunhofer phase approximation for strongly incoherent fields.

During the next quarter, the literature will be searched for data on large and small scale roughness, sea surface spectra, and the relation of the resulting statistics to measurable environment parameters such as wave height and/or wind speed. This will allow model input statistics to be defined in terms of the environmental parameters. In addition, the backscattering model will be modified to include time dependence.

III. CONVERGENCE ZONES

A. Introduction

Convergence zones are regions of focused sound from a shallow source in deep water. The acoustic waves are focused at or near the surface by refraction at great depths. Convergence zones occur typically at range intervals of 80 kyd or less when the near bottom sound velocity is greater than the sound velocity near the surface. In general, the convergence zone interval depends on the velocity-depth profile and the location of source and receiver.² For example, in the Atlantic and Pacific Oceans, the critical depth is between 4000 and 5000 yd. The resulting convergence zones appear every 60 to 80 kyd. When the critical depth is around 2000 yd (as in the Mediterranean Sea³) the zones appear every 30 to 40 kyd.

Theoretical treatments of convergence zone phenomena are based on both ray and wave methods, but most examinations have used ray theory techniques. Useful summaries of ray theory methods for studying convergence zones have been given by Hale⁴ and Arase⁵.

Ray tracing yields a qualitative picture of the distribution of energy, and it also provides a way of observing easily the changing characteristics of convergence zones when the profile parameters and source depths are varied. A typical ray trace is shown in Fig. 4. The source was at a depth of 100 yd and the velocity-depth profile was specified by the Epstein function. Note that the critical depth was approximately 2000 yd and that the convergence zones occur about every 32 kyd.

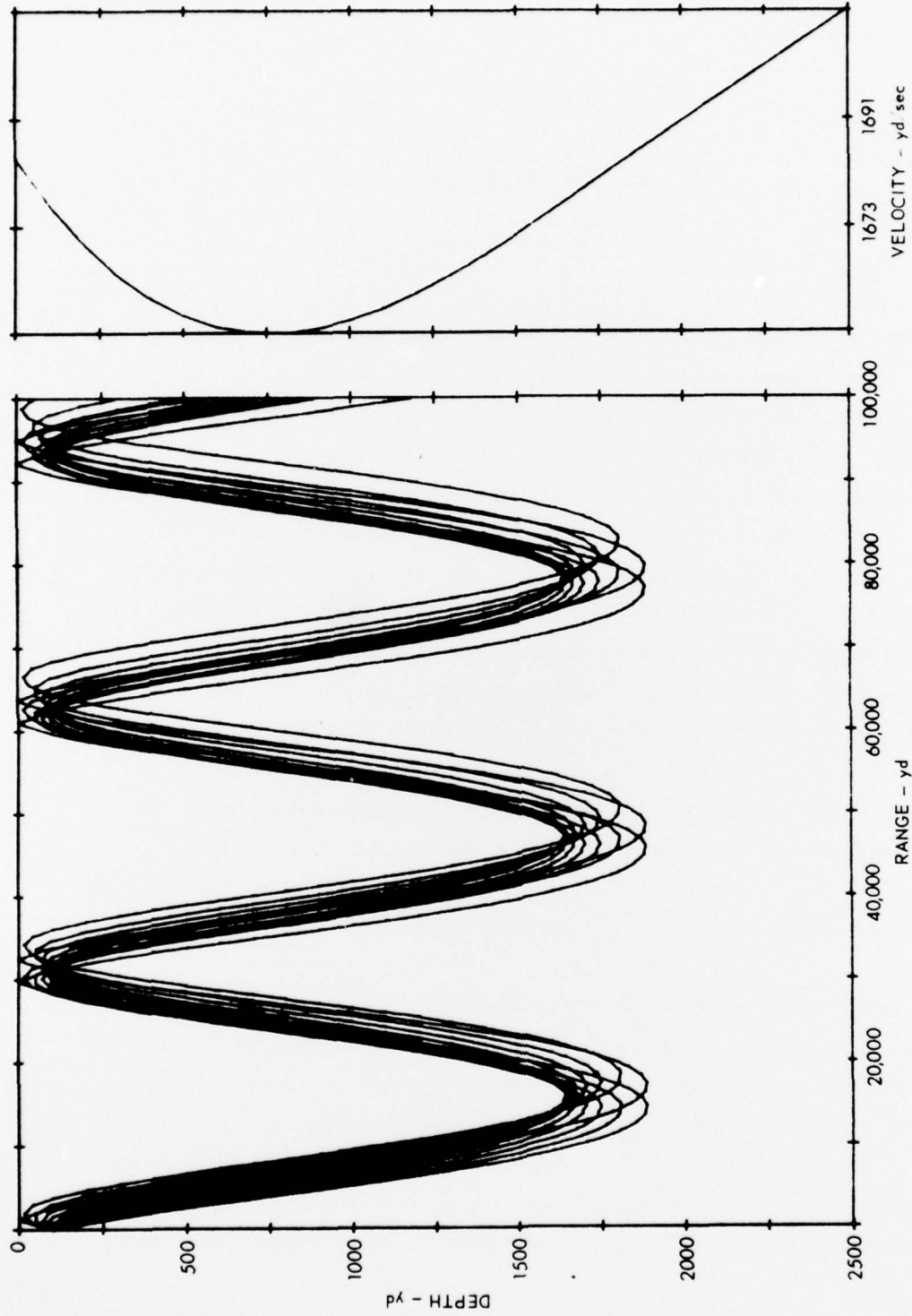


FIGURE 4
RAY TRACE DIAGRAM AND ASSOCIATED VELOCITY-DEPTH PROFILE

ARL - UT
AS-72-964
RLD - RFO
8 - 28 - 72

Ray methods can also give range predictions, but problems arise for intensity predictions due to the caustics (a caustic is defined as the locus of focal points at which adjacent rays touch each other). At caustics, ray theory intensity calculations go to infinity because $(\partial R/\partial \theta)$ goes to zero. In order to make ray theory intensity calculations in caustic regions, Pedersen and Gordon⁶ included various diffraction corrections in their calculations. They found that the correction derived by Brekhovskikh⁷ was superior to the correction derived by Marsh.⁸ These diffraction corrections allow ray theory intensity calculations to be made in both caustic regions and in shadow zone regions.

When normal mode methods are applied to convergence zone propagation, there are, in general, computational problems due to the large number of trapped modes. There is also the problem of finding a velocity-depth profile which permits the depth-dependent differential equation to be solved in terms of functions which can be calculated. Figure 5 shows a wave theory plot of transmission loss versus range for the Epstein profile of Fig. 4. The frequency was 10 Hz with 15 trapped modes. For higher frequencies, many more modes are trapped and the usual computational problems arise. There is however qualitative agreement between Figs. 4 and 5.

Since ray theory and conventional wave theory are both limited, several authors have attempted using WKB (Wentzel-Kramers-Brillouin) techniques. Bartberger and Ackler⁹ have been able to use WKB methods for convergence zone calculations at frequencies up to 300 Hz. Also Leibiger and Lee¹⁰ have applied WKB methods for convergence zone calculations up to 5 kHz.

In this section a brief outline will be given of Leibiger's method utilizing a more general Green's function. The basic idea is to transform the usual slowly converging normal mode expansion into an alternate, more rapidly converging series. Such a representation

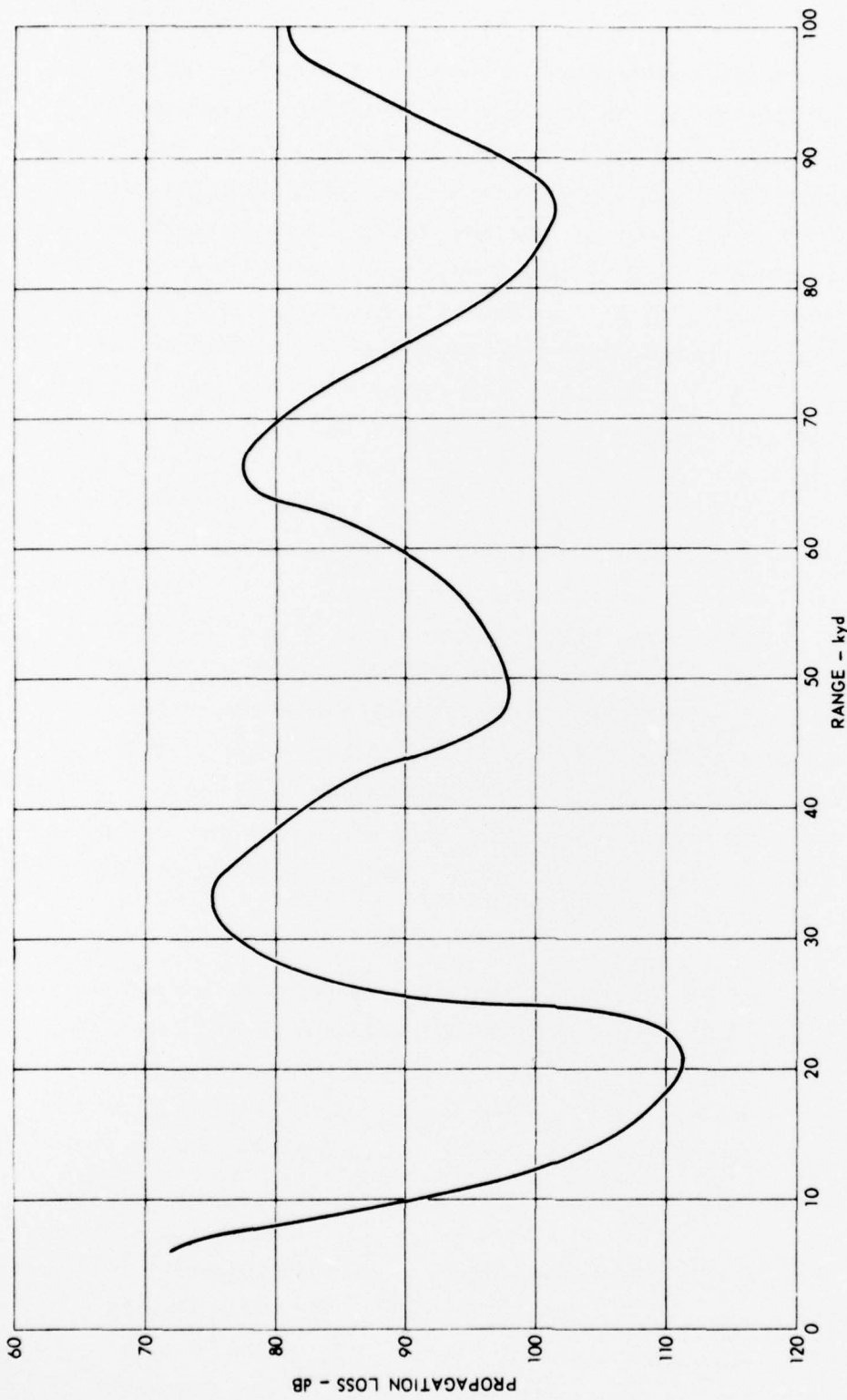
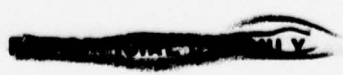


FIGURE 5
 PROPAGATION LOSS vs RANGE FOR SOURCE AND RECEIVER
 AT 100 yd DEPTH AND FREQUENCY OF 10 Hz

ARL - UT
 AS - 72 - 965
 RLD - DR
 8 - 10 - 72



was derived by Bremmer¹¹ by considering the total field to be made up of a sum of multipaths or hops. The ray or hop series was obtained by expanding the integrand (the inverse of the Wronskian) of the basic contour integral. Individual integrals were then evaluated to yield the hop series. Leibiger rederived Bremmer's work in his doctoral dissertation and has applied his techniques to many of the propagation modes encountered in the ocean. In the next section the Bremmer-Leibiger method will be discussed using Green's function.

B. Green's Function Expansion

The basic contour integral is given by¹²

$$P(r, z, z_0) = \oint G(z, z_0) H_0^1(\sqrt{r}) \xi d\xi \quad , \quad (62)$$

where P represents the acoustic pressure, r is the range coordinate, and z is the depth coordinate. The Green's function $G(z, z_0)$ is given by

$$G(z, z_0) = \frac{n_1(z_<) + R_1(z_1) \left[\frac{n_1(z_1) n_2(z_<)}{n_2(z_1)} \right] \left[n_2(z_>) + R_2(z_2) \frac{n_1(z_>) n_2(z_2)}{n_1(z_2)} \right]}{\omega(n_2, n_1) \left[1 - R_1(z_1) R_2(z_2) \frac{n_1(z_1) n_2(z_2)}{n_1(z_2) n_2(z_1)} \right]} \quad , \quad (63)$$

where the reflection coefficients $R_1(z_1)$ and $R_2(z_2)$ are defined at the boundaries z_1 and z_2 . Other functions and parameters are defined in Ref. 12 and are omitted for brevity.

When the WKB approximation is applied to the denominator of Eq. (63), the ratio $n_1(z_1)n_2(z_2)/n_1(z_2)n_2(z_1)$ is replaced by

$$\exp\left(-2ik_0 \int_{z_1}^{z_2} \left[n^2(z) - \cos^2 \theta_m \right]^{1/2} dz\right) \quad (64)$$

The relevant function to be expanded in Eq. (63) thus becomes

$$\left[1 - R_1(z_1)R_2(z_2) e^{-2ik_0 \int_{z_1}^{z_2} []^{1/2} dz} \right]^{-1} \quad (65)$$

When the expansion of Eq. (65) is used in the fundamental contour integral of Eq. (62), the acoustic field is represented by an infinite sum of integrals. In and near any particular convergence zone only a small subset of these integrals contributes in a significant way to the total sum. A great saving of effort is achieved by evaluating the integrals rather than the mode sum, especially at intermediate and high frequencies. The integrals are so ordered that each contributing integral can be associated with a particular multipath of the convergence zone.

Next quarter the multipath integrals defined by the series of Eq. (65) will be given explicitly and discussed.

REFERENCES

1. M. L. Boyd and R. L. Deavenport, "Forward and Specular Scattering from a Rough Surface: Theory and Experiment," to appear in *J. Acoust. Soc. Amer.*, January 1973.
2. R. J. Urick, "Caustics and Convergence Zones in Deep-Water Sound Transmission," *J. Acoust. Soc. Amer.* 38, 348-358 (August 1965).
3. C. C. Leroy, "Sound Propagation in the Mediterranean Sea," in *Underwater Acoustics*, V. M. Albers, Ed. (Plenum Press, New York, 1967), Vol. 2, pp. 203-341.
4. F. E. Hale, "Long-Range Sound Propagation in the Deep Ocean," *J. Acoust. Soc. Amer.* 33, 456-464 (April 1961).
5. T. Arase, "Some Characteristics of Long-Range Explosive Sound Propagation," *J. Acoust. Soc. Amer.* 31, 588-595 (May 1959).
6. M. A. Pedersen and D. F. Gordon, "Normal-Mode and Ray Theory Applied to Underwater Acoustics Conditions of Extreme Downward Refraction," *J. Acoust. Soc. Amer.* 51, 323-368 (January 1972).
7. L. M. Brekhovskikh, *Waves in Layered Media* (Academic Press, New York, 1960), pp. 474-492.
8. H. W. Marsh, "The Use of Ray Methods and First-Order Diffraction Corrections," Tech. Memo 1100-61-54, Navy Underwater Sound Laboratory, New London (1954).
9. C. L. Bartberger and L. L. Ackler, "Computer Programs for Normal Mode Propagation," Proc. 27th Navy Symposium on Underwater Acoustics, 28-30 October 1969, San Diego, California, Vol. II, pp. 501-518.
10. G. A. Leibiger and D. Lee, "Application of Normal Mode Theory to Convergence Zone Propagation," Vitro Lab. Research Mem. VL-8512-12-0, Vitro Laboratories, West Orange (30 November 1968).
11. H. Bremmer, *Terrestrial Radio Waves* (Elsevier, New York, 1949).
12. R. L. Deavenport, "A Normal Mode Theory of an Underwater Acoustic Duct by Means of Green's Function," *Radio Sci.* 1, 709-724 (June 1966).

12 September 1972

DISTRIBUTION LIST FOR
QUARTERLY PROGRESS REPORT No. 4
UNDER CONTRACT N00024-71-C-1266
1 April - 30 June 1972

Copy No.

1 Commander
Naval Ship Systems Command
Department of the Navy
Washington, D. C. 20360
Attn: PMS 302-44

2 PMS-387

3 - 4 Technical Library (Code 2052)

5 Commander
Naval Undersea Center
San Diego, California 92132
Attn: Code 503

Director
Naval Research Laboratory
Department of the Navy
Washington, D. C. 20390

6 Attn: Code 8120

7 Code 8172

8 - 9 Officer-in-Charge
New London Laboratory
Naval Underwater Systems Center
New London, Connecticut 06320
Attn: Code TALL

Commanding Officer and Director
Naval Coastal Systems Laboratory
Department of the Navy
Panama City, Florida 32401

10 Attn: Code 700

11 Code 720

12 Superintendent
Naval Postgraduate School
Monterey, California 93940
Attn: Prof. H. Medwin

Distribution List for QPR No. 4 under Contract N00024-71-C-1266 (Cont'd)

Copy No.

13 - 14	Commanding Officer and Director Defense Documentation Center Defense Services Administration Cameron Station, Building 5 5010 Duke Street Alexandria, Virginia 22314
15	Office of Naval Research Resident Representative Room No. 582 Federal Building Austin, Texas 78701
16	Garland R. Barnard, ARL/UT
17	Michael L. Boyd, ARL/UT
18	Roy L. Deavenport, ARL/UT
19	Harlan G. Frey, ARL/UT
20	Sam A. Means, ARL/UT
21	Patrick J. Welton, ARL/UT
22	Library, ARL/UT
23 - 24	ARL Reserve

DOCUMENT CONTROL DATA - R & D

Security classification of title, body of abstract and indexing annotation must be entered when the overall report is classified

1. ORIGINATING ACTIVITY (Corporate author) Applied Research Laboratories The University of Texas at Austin Austin, Texas 78712		2a. REPORT SECURITY CLASSIFICATION UNCLASSIFIED, FOUO	
		2b. GROUP	
3. REPORT TITLE QUARTERLY PROGRESS REPORT No. 4 UNDER CONTRACT N00024-71-C-1266			
4. DESCRIPTIVE NOTES (Type of report and inclusive dates) quarterly report, 1 April - 30 June 1972			
5. AUTHOR(S) (First name, middle initial, last name)			
6. REPORT DATE 12 September 1972		7a. TOTAL NO. OF PAGES 37	7b. NO. OF REFS 12
8a. CONTRACT OR GRANT NO. N00024-71-C-1266		9a. ORIGINATOR'S REPORT NUMBER(S) —	
b. PROJECT NO. SF 11552002, Task 8118		9b. OTHER REPORT NO(S) (Any other numbers that may be assigned this report) —	
c.			
d.			
10. DISTRIBUTION STATEMENT FOR OFFICIAL USE ONLY			
11. SUPPLEMENTARY NOTES —		12. SPONSORING MILITARY ACTIVITY Naval Ship Systems Command Department of the Navy Washington, D. C. 20360	
13. ABSTRACT This quarter the reflection and scattering models were further developed, and a review of the literature preliminary to the development of a convergence zone propagation model was completed. (U-FOUO) In Section II, expansion of the heuristic scattering model to include composite (both large and small scale roughness) surface statistics is given which should improve backscattering predictive capabilities. This model does not include slope correction terms but has the advantage of simplicity. The more rigorous theoretical model which includes slope corrections terms is also expanded to allow for composite surface roughness. (U-FOUO) A survey of the literature covering convergence zone propagation is summarized in Section III. An approach is outlined for the development of a convergence zone model using a Green's function expansion. This technique results in an ordered integral expansion where each integral can be associated with a particular multi-path. (U-FOUO)			

14 KEY WORDS	LINK A		LINK B		LINK C	
	ROLE	WT	ROLE	WT	ROLE	WT
Composite surfaces Convergence zones Slope Corrections Surface scattering						

APPLIED
RESEARCH
LABORATORIES
THE UNIVERSITY OF TEXAS
AT AUSTIN

